

# Quantum cascade lasers for the 8- $\mu\text{m}$ spectral range: technology, design, and analysis

V V Dudelev, E D Cherotchenko, I I Vrubel, D A Mikhailov, D V Chistyakov, V Yu Mylnikov, S N Losev, E A Kognovitskaya, A V Babichev, A V Lutetskiy, S O Slipchenko, N A Pikhin, A G Gladyshev, K A Podgaetskiy, A Yu Andreev, I V Yarotskaya, M A Ladugin, A A Marmalyuk, I I Novikov, V I Kuchinskii, L Ya Karachinsky, A Yu Egorov, G S Sokolovskii

DOI: <https://doi.org/10.3367/UFNe.2023.05.039543>

## Contents

1. Introduction	92
2. Quantum cascade lasers with high power characteristics	93
3. Investigation of threshold and volt- and watt-ampere characteristics	94
4. Investigation of temperature influence on the output characteristics of quantum cascade lasers	95
5. Conclusions	97
References	98

**Abstract.** Quantum cascade lasers (QCLs) have received enormous attention from the scientific community due to their broad range of applications in a wide variety of industries, agriculture, healthcare, environmental protection, and many other scientific and technical fields. In this article, in addition to a review of the main applications and the state of research and development of high-power QCLs in the mid-infrared range, we consider the features of their manufacturing technology that make it possible to obtain a high peak power and discuss the effect of overheating of the active region on the output optical power and spectral characteristics. A comparison is made of the characteristics of QCLs with the same cavity parameters but with different active regions made on the basis of substrate-matched or strained heteropairs, which provides a different energy barrier between the upper laser level and the continuum. It is shown that the use of strained heteropairs in the active region of a QCL

provides an almost twofold increase in the characteristic temperature  $T_0$  as well as a significantly higher efficiency and an increase in the maximum output optical power to over 21 W, which is a world record for a single stripe QCL with a 8  $\mu\text{m}$  spectral range.

**Keywords:** quantum cascade laser, heterostructure, mid-infrared range, chirp, heat sink

## 1. Introduction

Quantum cascade lasers are unique devices that allow efficient generation of radiation in the mid-infrared range, which is of particular interest due to the presence of many intense molecular absorption lines associated with vibrational and rotational degrees of freedom, as well as due to two atmospheric transparency windows in the regions of 4–5 and 8–14  $\mu\text{m}$ . The combination of unique properties of QCLs, such as compactness and efficiency, in combination with spectral characteristics, makes possible their use in a wide variety of industries, agriculture, healthcare, environmental protection, and many other areas, as shown schematically in Fig. 1. Separately, we can highlight the use of QCLs in solving a number of pressing problems in medical diagnostics [1], environmental monitoring [2, 3], and technological processes using gas spectroscopy techniques [4–6]. Developments are also underway for the use of QCLs in biomedicine [7, 8], the fight against terrorism [6, 9], and the development of secure noise-resistant optical communication channels, primarily in atmospheric transparency windows in the mid-IR range [10–12].

The idea of QCLs was first proposed by Kazarinov and Suris in 1971 [13], who described a unipolar device based on a superlattice and generating radiation due to intraband electronic transitions in the conduction band when a potential is applied to the structure. In the unipolar device, one electron takes part in the production of several photons by tunneling into an adjacent cascade followed by a laser transition. This principle is fundamentally different from the standard method

V V Dudelev<sup>(1,\*), E D Cherotchenko<sup>(1), I I Vrubel<sup>(1), D A Mikhailov<sup>(1), D V Chistyakov<sup>(1), V Yu Mylnikov<sup>(1), S N Losev<sup>(1), E A Kognovitskaya<sup>(1), A V Babichev<sup>(1), A V Lutetskiy<sup>(1), S O Slipchenko<sup>(1), N A Pikhin<sup>(1), A G Gladyshev<sup>(2), K A Podgaetskiy<sup>(3), A Yu Andreev<sup>(3), I V Yarotskaya<sup>(3), M A Ladugin<sup>(3), A A Marmalyuk<sup>(3), I I Novikov<sup>(2,4), V I Kuchinskii<sup>(1), L Ya Karachinsky<sup>(2,4), A Yu Egorov<sup>(2,5), G S Sokolovskii<sup>(1)</sup></sup></sup></sup></sup></sup></sup></sup></sup></sup></sup></sup></sup></sup></sup></sup></sup></sup></sup></sup></sup></sup></sup>

<sup>(1)</sup> Ioffe Institute, Russian Academy of Sciences, ul. Politekhnicheskaya 26, 194021 St. Petersburg, Russian Federation

<sup>(2)</sup> Connector Optics LLC, ul. Domostroitel'naya 16B, 194292 St. Petersburg, Russian Federation

<sup>(3)</sup> Polus Research Institute of M.F. Stelmakh Joint Stock Company, ul. Vvedenskogo 3, korp. 1, 117342 Moscow, Russian Federation

<sup>(4)</sup> ITMO University, Kronverkskii prosp. 49, 197101 St. Petersburg, Russian Federation

<sup>(5)</sup> Alferov St. Petersburg National Research Academic University, Russian Academy of Sciences, ul. Khlopina 8, korp. 3A, 194021, St. Petersburg, Russian Federation  
E-mail: <sup>(\*)</sup> v.dudelev@mail.ru

Received 22 May 2023

*Uspekhi Fizicheskikh Nauk* 194 (1) 98–105 (2024)

Translated by V N Ragozin

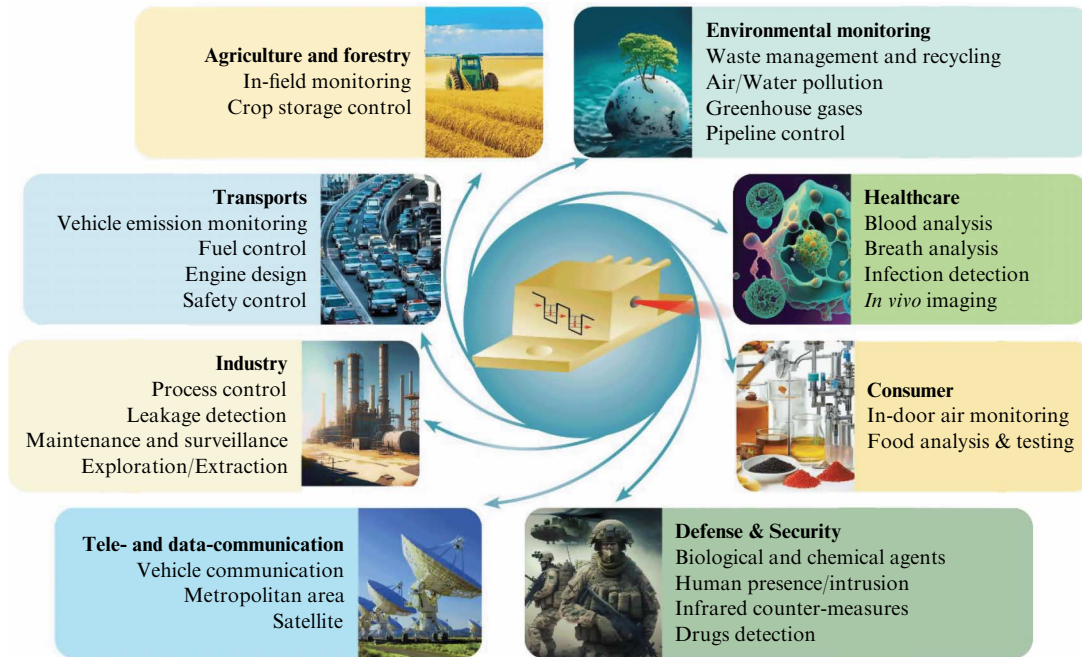


**Figure 1.** Schematic representation of various applications of QCLs.

of generating radiation in semiconductor lasers, where the recombination of a conduction band electron with a hole in the valence band produces only one photon.

Despite the apparent simplicity of the idea, the practical implementation of QCLs became possible only in 1994 [14]; this is due to the special features of electron dynamics in nanoscale layers, wherein the rate of phonon relaxation at heterointerfaces significantly exceeds the rate of radiative transitions, which calls for the construction of complex heterostructures that provide fast depopulation of the lower laser level to achieve population inversion. The combination of the specified conditions leads to an extremely high technological complexity of heterostructures consisting of thousands of nanoscale layers combined into tens or even hundreds of identical cascades.

The unrelenting interest in QCLs, despite their high technological complexity, is largely due to the fact that lasing in the mid-infrared range with conventional interband semiconductor lasers at room temperature is significantly hampered due to the properties of the band structure of narrow-gap semiconductors, which leads to a rapid increase in nonradiative Auger recombination with increasing lasing wavelength. This limits their use to maximum wavelengths of about 4  $\mu\text{m}$ . An alternative and effective source of IR radiation is interband cascade transition lasers (ICLs), in which charge carriers recombining in the active region of the cascade tunnel from cascade to cascade due to the presence of third-order heterojunctions. In this case, the radiation wavelength in ICLs, as well as in diode lasers, depends on the band gap of the interband transition, which is ultimately determined by the chemical composition of the material of the active region, which limits their operating spectral range. At room temperature, which is of particular interest for practical applications, it is limited to 3–7  $\mu\text{m}$  [15–17]. For comparison, the QCL emission wavelength is determined by the position of size quantization levels in the conduction band and is controlled by changing the thickness of quantum wells without changing the composition of the material inside the

heterostructure, significantly expanding the possible lasing spectrum. Specifically, in a room-temperature QCL, it is possible to achieve radiation at wavelengths approaching 20  $\mu\text{m}$  [18, 19] and up to 25  $\mu\text{m}$  [20] with slight cooling (240 K). A separate and important advantage of QCL structures is the ability to obtain terahertz radiation with wavelengths of the order of several hundred microns [21] with significant power [22]. Despite the fact that, so far, applications of QCLs in this spectral region are mainly limited by the need to operate at low temperatures, recent publications have shown both the fundamental possibility of using thermoelectric cooling at temperatures of 196 K [23] and 210 K [24] and operation at 250 K [25]. At room temperature, the generation of terahertz radiation with a power of up to several milliwatts by QCLs is possible due to intracavity generation of the difference frequency with an artificial increase in the second-order nonlinearity in the structure [26, 27].

Since 1994, QCL technology has undergone enormous changes. Current performance values are the result of continuous improvements in design, quality of materials, and manufacturing technology, which is reflected in operating temperatures, threshold currents, output powers, and spectral and spatial characteristics of the output radiation. In this paper, we consider the features of QCL manufacturing technology that make it possible to obtain high peak powers and discuss some fundamental factors affecting the CW laser mode. To do this, we carried out comparative investigations of the characteristics of QCLs for the spectral range of 8  $\mu\text{m}$  grown on an indium phosphide substrate, whose active regions are based on heteropairs of different chemical compositions and provide different values of the energy barrier between the upper laser level and the continuum.

## 2. Quantum cascade lasers with high power characteristics

As with any laser, the applicability of a QCL for solving a particular problem is determined by several parameters, such

as beam divergence, lasing efficiency, threshold current density, output power, and spectral radiation composition. Depending on the type of use, these parameters have different requirements and, accordingly, the laser design undergoes corresponding changes to meet the final purpose. A significant portion of applications require a high output power. Figure 2 depicts the highest peak powers of room-temperature QCLs as a function of wavelength.

The best results were achieved in the wavelength range of 4.5–5  $\mu\text{m}$ . At the same time, obtaining a high power in this spectral range requires new approaches to the design of both the waveguide and the active region. Initially, the need to apply a high voltage to align energy levels in the system of cascades before the laser starts operating and a high pump current density imply significant heating of the device during the lasing process, which, in turn, leads to radiation degradation. When using a cascade of *lattice-matched* (hereinafter referred to as ‘matched’) InGaAs/InAlAs heteropairs, in which the lattice parameters of the well and barrier coincide with the InP, the energy gap at the heterointerface is 520 meV [46], which exceeds the photon energy in this spectral range by only a factor of 2, inevitably leading to an insufficient barrier at the upper laser level and, as a consequence, to significant leakage of charge carriers into the continuum. The use of *strain-compensated* heteropairs, in which the well and the barrier are mismatched with InP in the lattice parameter but mutually compensate for the resultant strain, has made it possible to significantly improve the characteristics of QCLs for the 4.5–5  $\mu\text{m}$  spectral range. Specifically, based on strain-compensated heteropairs, QCLs with improved efficiency were obtained in [47], and over 120 W in pulsed mode was obtained for QCLs with a stripe width of 400  $\mu\text{m}$  [30]. The idea was developed through the use of strained heteropairs for the active region, where the well and barrier are mismatched with InP and do not compensate for the resultant strain, to remove which one uses the of damping layers matched to the substrate. Thus, the use of strained heteropairs with AlAs inserts made it possible to produce QCLs with a record low temperature dependence of the threshold current [48], as well as to obtain record efficiency [49] and output power [31]. Furthermore, in Refs [30, 31], along with high power, QCLs have a relatively high threshold current density and a large divergence of the laser beam. When the structure maintains a

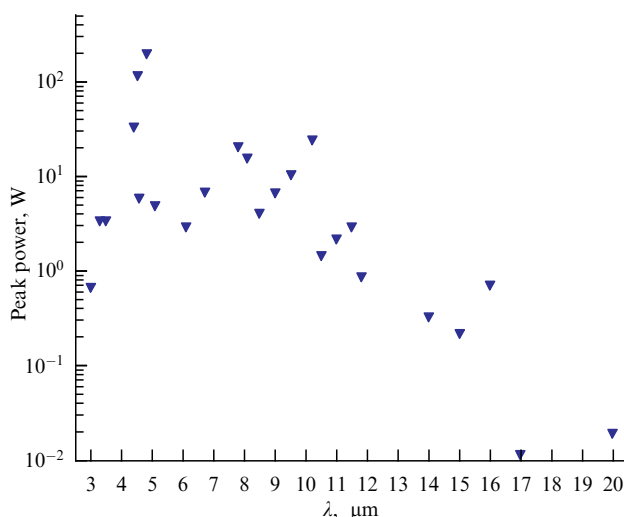


Figure 2. Peak powers of QCLs in relation to the laser wavelength [19, 28–45].

balance of threshold and power characteristics, as well as beam quality, the peak power varies from tens of watts to fractions of a watt with increasing wavelength. The latter is associated with approaching the phonon absorption zone, where it is basically impossible to achieve lasing. At the same time, significant progress has been observed in the area of the second transparency window: tens of watts for  $\lambda \sim 8 \mu\text{m}$  and  $\lambda \sim 10 \mu\text{m}$  [35, 39], which in the future can be used for wireless communications.

For QCLs in the spectral range of 8–10  $\mu\text{m}$ , the photon energy becomes 0.4–0.5 times that for 4.5–5- $\mu\text{m}$  range lasers, which makes it possible to construct high-power QCLs with active regions based on matched heteropairs. In particular, for QCLs using matched heteropairs, record peak powers of 16 [35] and 25 W [39] was obtained for lasers with stripe widths of 60 and 95  $\mu\text{m}$ , respectively. At the same time, significant interest persists in producing new active regions on strained or strain-compensated heteropairs to improve the output characteristics of QCLs in this spectral range. The power characteristics of QCLs are largely determined by optical losses, the rate of heat removal from the active region, and the efficiency of current pumping. The last is influenced by two main temperature-determined processes: the reverse current associated with the thermal influx of carriers from the injector level to the lower laser level of the previous cascade, which reduces the population inversion, and the escape of carriers into the continuum, leading to a parasitic leakage current. Since the heating of the active region increases with the pump current, even in the pulsed mode [35], this problem becomes especially urgent for high-power QCLs. As already indicated above, the gap in the conduction band for a matched heteropair is 520 meV, which makes it possible to obtain a sufficient energy gap of  $\sim 130$ –160 meV between the injector level and the lower laser level to suppress the reverse current, as was shown in Refs [50, 51]. In this case, for a QCL with a spectral range of 8  $\mu\text{m}$ , the energy barrier between the upper laser level and the continuum is about 100 meV, which does not allow this leakage channel to be completely suppressed. At the same time, to suppress the reverse current under similar conditions, the use of strained  $\text{Al}_{0.63}\text{In}_{0.37}\text{As}/\text{Ga}_{0.35}\text{In}_{0.65}\text{As}$  heteropairs makes it possible to significantly increase the energy gap in the conduction band at the heterointerface to 740 meV [52, 53], which provides a significantly wider energy barrier preventing the escape of carriers into the continuum. Therefore, designing the active region of a QCL for the spectral range of 8  $\mu\text{m}$  based on strained heteropairs potentially makes it possible to reduce the thermal leakage current and increase the efficiency and output power of QCLs, but the epitaxial growth of such lasers is more complex, since it requires additional layers to compensate for the strain.

### 3. Investigation of threshold and volt- and watt-ampere characteristics

We have developed and manufactured QCLs with active regions based on heteropairs, both strained (type 1) and matched (type 2) with an InP substrate, and studied the characteristics of these QCLs for the spectral range  $\lambda \sim 8 \mu\text{m}$ . Epitaxial growth was two-stage: the active region was grown by molecular beam epitaxy, and the upper waveguide plate was grown by metal-organic vapor phase epitaxy. The active region of QCLs with strained layers contained 40 quantum cascades, a layer-by-layer description

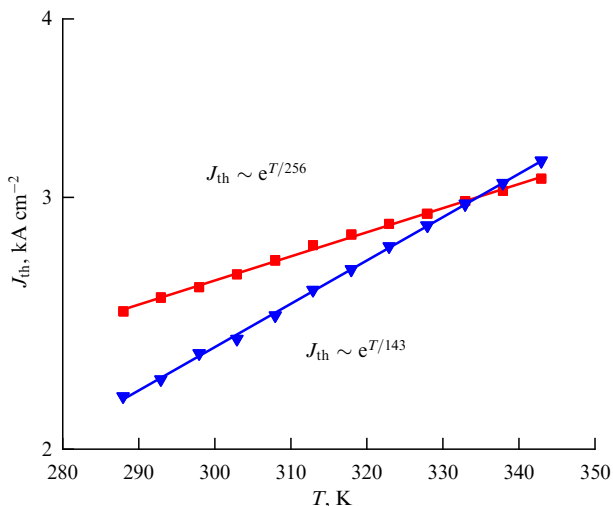


**Figure 3.** Temperature dependence of QCL threshold current density. Dependence is plotted on a logarithmic scale on the threshold current density scale. Straight red line: type 1; straight blue line: type 2.

of which is given in Ref. [52]. The QCL heterostructure with an active region based on a matched heteropair consisted of 50 quantum cascades. A complete description of this structure is given in Ref. [35].

The grown heterostructures were subjected to post-growth processing, which included the following operations: applying a photoresist mask, etching grooves through it to form a stripe contact (hereinafter referred to as stripes) in the form of a ridge waveguide, applying a dielectric, opening the contact windows, and sputtering the upper and lower contacts. A detailed description of the post-growth process is given in Ref. [54]. Next, the heterostructure was divided into chips, which were mounted on copper heat sinks with the epitaxial layer down. For the studies, we used QCLs with stripe widths of 10–50  $\mu\text{m}$  and resonator lengths of  $\sim 3$ –5 mm. QCL mirrors were formed by cleavages along the crystallographic axes.

The QCLs were studied under pumping by current pulses with a duration of  $\sim 100$  ns and a repetition rate of 11.5 kHz. An investigation was made of the temperature dependences of threshold QCL current densities in the range of 298–343 K. The research results are presented in Fig. 3, where the temperature dependence of the threshold current density is

plotted on a logarithmic scale. The linear approximation of this dependence allows us to find the characteristic temperature  $T_0$ , which determines the rate of increase in the threshold current density with temperature in accordance with the empirical expression

$$J_{\text{th}} \sim \exp\left(\frac{T}{T_0}\right), \tag{1}$$

where  $J_{\text{th}}$  is the threshold current density and  $T$  is the temperature. The resultant values of the characteristic temperature were 256 and 143 K for type 1 and type 2 structures, respectively, which indicates a decrease in heat leakage in the structures with strained layers.

The results of studying the current-voltage and watt-ampere characteristics of a QCL with a stripe width of 50  $\mu\text{m}$  and a resonator length of 5 mm are presented in Fig. 4. The current-voltage characteristic of the type 1 QCL (blue curve in Fig. 4) shows a reduction in operating voltage of  $\sim 20\%$  compared to the type 2 QCL, which is proportional to the reduction in the number of cascades. Studies of watt-ampere characteristics (red curves) have shown that QCLs with an active region based on strained heteropairs have a higher maximum optical output power: more than 21 W (a world record for this wavelength) versus 14 W for QCLs with a matched heteropair. As one can see from the measurement data in Fig. 4, for QCLs with the same geometric parameters, the use of strained heteropairs in the active region leads to a threefold increase in the differential efficiency  $\eta$ , which is determined from the slope of the watt-ampere characteristic:  $1.2 \text{ W A}^{-1}$  versus  $0.42 \text{ W A}^{-1}$ . Reducing the operating voltage, as well as increasing  $\eta$ , made it possible to obtain a significant increase in laser efficiency of 12.7% versus 4.4% for type 1 and type 2 devices, respectively.

Therefore, the studies performed suggest that the use of an active region based on strained heteropairs makes it possible to increase the output characteristics of QCLs, as well as moderate the temperature dependence of the threshold current.

#### 4. Investigation of temperature influence on the output characteristics of quantum cascade lasers

As shown in Ref. [55], it is the heating of the active region that is the main factor affecting the maximum output power for

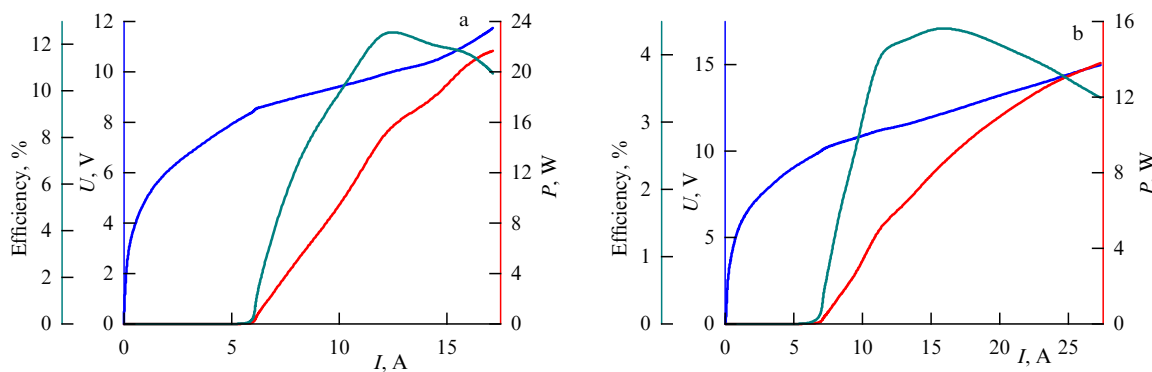


**Figure 4.** Efficiency and watt- and volt-ampere laser characteristics for two types of structures with stripe width of 50  $\mu\text{m}$  and resonator length of 5 mm: (a) strained heteropairs (type 1), (b) matched heteropairs (type 2).

both pulsed and continuous pumping modes. Simulations using the heat conduction equation shows that the leakage of Joule heat from the active region into the plates begins roughly 100 ns from the beginning of the pulse. The heating of the outer plates takes tens of microseconds until an equilibrium thermal distribution in the device sets in, which is consistent with experimental data. Overheating of the active region is directly related to its thermal conductivity, which depends on two factors: the presence of interfaces between the heterostructure layers and the composite chemical composition of the layers, which in most cases for QCLs are three-component solid solutions or binary compounds [56]. These features of the active region of the laser are characterized by effective phonon diffusion retardation by the roughness of the layer interface and the presence of scattering isovalent substitutions in the solid solution lattice. In this case, it is the second factor that is the key in the deterioration of thermal conductivity [56], and therefore represents a fundamental limitation for the temperature mode of QCL operation. If overheating of the active region and the corresponding shift in threshold characteristics do not lead to complete degradation of laser radiation, it is possible to achieve a continuous operating mode. However, even within these fundamental limitations, a suitable structure design and correct heat sink [57] allow one to obtain impressive results: high power characteristics with a high beam quality.

Primary heating of the active region can be investigated by the shift of the laser line during the development of the pump pulse: this is so-called linear frequency modulation (chirp) [58, 59]. The chirp is directly proportional to the QCL heating rate [35]:

$$\frac{dT}{dt} = \frac{dn}{dt} \left( \frac{dn}{dT} \right)^{-1} = \frac{n}{\lambda_m} \frac{d\lambda_m}{dt} \left( \frac{dn}{dT} \right)^{-1}, \quad (2)$$

where  $T$  is temperature,  $t$  is time,  $n$  is the refractive index,  $dT/dt$  is the heating rate of the active region,  $d\lambda_m/dt$  is the chirp, and  $dn/dT$  is the variation rate of the refractive index with temperature. By measuring the chirp, it is possible to show how quickly the QCL heats up during the development of the pump pulse. It is important to note here that comparing chirp measurement data with expression (2) is not a trivial task. Measuring the change in the refractive index with temperature  $dn/dT$  requires either ultrahigh resolution instruments to make possible measuring the temperature-

induced wavelength change with  $d\lambda_m/dt$  in a narrow wavelength range or structures that have about a hundred Fabry–Perot modes in the spectrum. A careful theoretical analysis of expression (2) allows us to make estimates for this factor, which, in combination with thermal conduction equation simulations, lead to a reasonable calculation of the amount of overheating of the active region during the pulse.

We conducted experimental studies of the time-resolved spectra of type 1 and type 2 QCLs. As can be seen from the results shown in Fig. 5, a shift in the laser line is observed during the development of the pulse. The chirp value was determined for both QCL types for pump current amplitudes of 10 and 15 A. While at a current of 10 A it was  $0.2 \text{ \AA ns}^{-1}$  and  $0.24 \text{ \AA ns}^{-1}$  for type 1 and type 2 QCLs, respectively, with an increase in the pump current by 1.5 times, the chirp values were already  $0.31 \text{ \AA ns}^{-1}$  and  $0.41 \text{ \AA ns}^{-1}$ . Research data show that QCLs with a matched heteropair active region heat up at a significantly higher rate, especially for pump currents exceeding  $1.5 I_{th}$ .

As shown in Ref. [57], improving heat removal from the side regions of the ridge waveguide can significantly reduce the overheating of the structure. In this case, for continuous and quasi-continuous modes, the main overheating of the active region relative to the environment is due to the heating in the first microseconds of laser operation, when the heat generated in the active region does not have time to be removed from it. The temperature dependence of the threshold current will also affect the heating rate of the QCL active region. That is, the implementation of such oscillation modes calls for appropriate optimization to reduce the leakage currents and, accordingly, the heating of the active region, which is much easier to implement using structures with strained heteropairs.

Using a type 1 QCL with an optimized cavity design that ensures heat removal from the side walls of the active region, investigations were made of the effect of active region heating on the output optical power. We studied the emission pulses of a QCL pumped by current pulses of various durations (Fig. 6). One can see that the current heating of the QCL is balanced by the rate of heat removal from the active region only 40–60  $\mu\text{s}$  after switching on, depending on the sample. In this case, the main decrease in intensity and, accordingly, an increase in the threshold current are observed in the first 3  $\mu\text{s}$  of the pulse.

Comparative studies of the output characteristics were carried out in pulsed (pump pulse duration:  $\sim 100 \text{ ns}$ ;

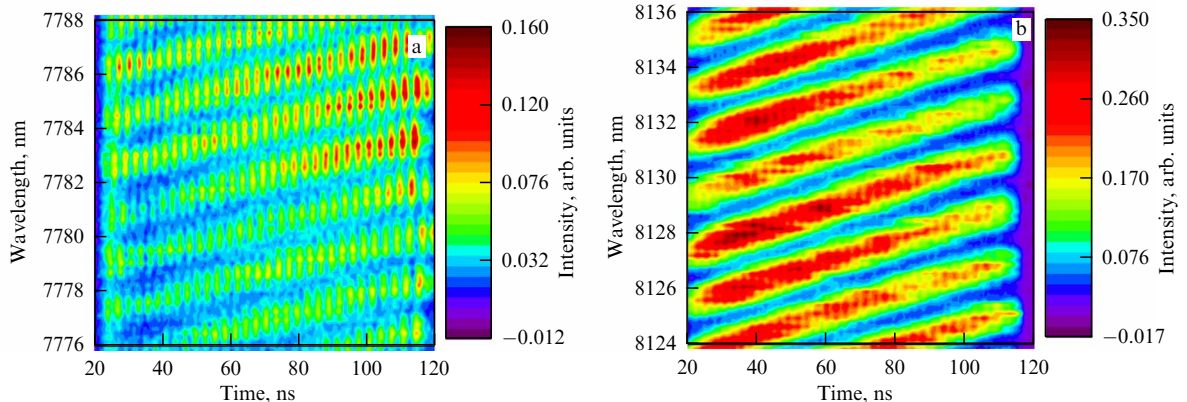


**Figure 5.** Time-resolved QCL spectra at a pump current amplitude of 15 A: (a) type 1 (b) type 2.

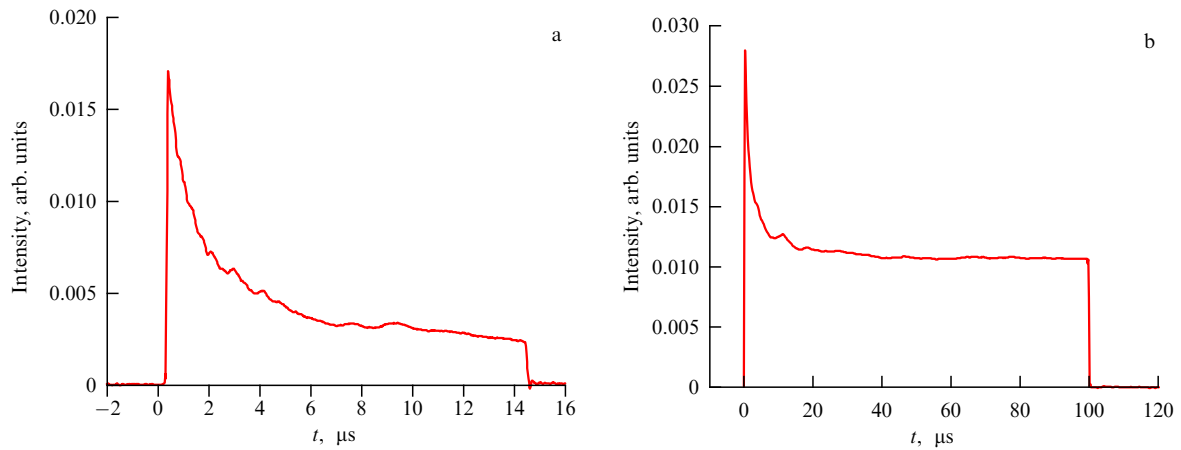


**Figure 6.** Oscillograms of a type 1 QCL radiation pulse with pump pulse durations of 14.5  $\mu\text{s}$  (a) and 100  $\mu\text{s}$  (b).

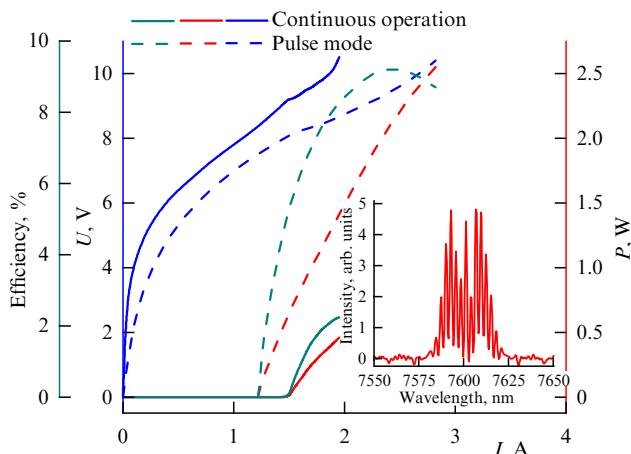


**Figure 7.** Characteristics of QCLs made from a type 1 heterostructure with a stripe width of 19  $\mu\text{m}$  and improved heat removal. Solid curves: CW mode. Dashed curves: pulse oscillation mode with a pulse length of  $\sim 100$  ns and repetition rate of 11.5 kHz. Blue curves are current-voltage characteristics, red curves are watt-ampere characteristics, and turquoise curves stand for efficiency. Inset shows the QCL emission spectrum in the CW mode at a pump current of 1.6 A.

repetition rate: 11.5 kHz) and continuous (CW) laser modes (Fig. 7). The presence of active region overheating in the CW mode is clearly visible from the increase in the threshold current value. The overheating of the active region at the threshold, based on estimates for the characteristic temperature  $T_0$ , is  $\sim 70$  K and continues to increase with the pump current, as indicated by a rapid bend in the watt-ampere characteristic compared to the pulsed mode, and a fivefold drop in the output power and efficiency of the QCL.

## 5. Conclusions

Summarizing the results obtained, several main conclusions can be drawn. The presence of tens of quantum cascades in the active region, which comprises several thousand nanoscale layers, determines the operation of QCLs at elevated voltages (usually over 10 V), as well as a relatively high series resistance in the linear portion of the watt-ampere characteristic. The fundamental problem of QCLs is therefore the Joule heat released in the active region, as well as its slow distribution throughout the rest of the structure until the attainment of equilibrium. Heating affects the decrease in

radiation intensity and leads to linear-frequency modulation of the laser line. The latter circumstance can be used for continuous spectral scanning, which shows promise for gas analysis with single-frequency QCLs. This effect is clearly demonstrated in QCLs developed on the basis of a type 2 structure with a U-shaped resonator produced by connecting waveguides in the shape of a semicircle and flat ridge waveguides [60]. However, for most other applications of QCLs, the need for rapid heat removal or a fundamental reduction in thermal influence is especially acute. Although the decrease in the temperature of the active region is fundamentally limited by the heat-conducting properties of the internal layers, properly organized heat removal, including from the side parts of the stripe, makes it possible to achieve thermal equilibrium and a continuous-wave operation. At the same time, the pulsed operating mode with pulse durations of the order of 100 ns is almost completely determined by the properties of the active region due to the fact that in such a short period of time the heat does not have time to go beyond its boundaries. The technology for measuring the heating rate of the active region, which involves measuring the chirp during heating, allows accurately determining the overheating in a specific structure, which is necessary for further analysis and optimization of parameters. At the same time, it does not have the disadvantages of temperature measurement technologies based on scanning a laser mirror, which do not provide information about thermal processes inside the laser.

A possible and effective solution to problems arising from the active region overheating is the use of strained layers that provide a significantly larger gap in the conduction band at the well/barrier heterointerface. This provides a reduction in the thermal emission of charge carriers from the active region into the continuum and a significant improvement in all operating characteristics of the QCL. A comparison of the characteristics of QCLs with the same cavity parameters, but with an active region based on matched and strained heteropairs, suggests that the use of this solution provides an almost twofold increase in the  $T_0$  parameter in the temperature dependence of the threshold current compared to QCLs based on heterostructures with unstrained layers, as well as a 50% increase in maximum output optical power. In particular, a peak power of over 21 W was obtained in the present work, which is a new world record for the 8- $\mu\text{m}$  spectral range for single stripe devices. The technology

described in this work also improves efficiency, which is due to the higher gain in structures with strained layers in the active region, while these characteristics are achieved with fewer cascades in the active region. The possible combination of growth technologies that improve electrical conductivity [35] with post-growth processing technologies that reduce heating opens up further prospects for increasing the power and efficiency of QCLs.

**Acknowledgments.** The research was supported by a grant from the Russian Science Foundation (project no. 21-72-30020).

## References

1. Vaks V L et al. *Proc. SPIE* **9934** 99340E (2016)
2. Cousin P et al., in *Instrumentation and Measurement Technologies for Water Cycle Management* (Springer Water, Eds A D Mauro, A Scozzari, F Soldovieri) (Cham: Springer, 2022) pp. 251–277, [https://doi.org/10.1007/978-3-031-08262-7\\_11](https://doi.org/10.1007/978-3-031-08262-7_11)
3. Nabiev S S, Palkina L A, in *The Atmosphere and Ionosphere: Elementary Processes, Monitoring, and Ball Lightning* (Physics of Earth and Space Environments, Eds V L Bychkov, G V Golubkov, A I Nikitin) (Cham: Springer, 2014) pp. 113–200, [https://doi.org/10.1007/978-3-319-05239-7\\_3](https://doi.org/10.1007/978-3-319-05239-7_3)
4. Moravek A et al. *Atmos. Meas. Tech.* **12** 6059 (2019)
5. Kolker D B et al., in *2022 Intern. Conf. Laser Optics, ICLO, 20–24 June 2022, Saint Petersburg, Russian Federation*, <https://doi.org/10.1109/ICLO54117.2022.9840076>
6. Kumar C, Patel N *Proc. SPIE* **8268** 826802 (2012)
7. Schwarm K K et al. *Appl. Phys. B* **126** 9 (2020)
8. Vaks V L et al. *Phys. Usp.* **57** 684 (2014); *Usp. Fiz. Nauk* **184** 739 (2014)
9. Takeuchi E B et al. *Proc. SPIE* **6741** 674104 (2007)
10. Yang K et al. *Electron. Lett.* **57** 665 (2021)
11. Gopinath S, Ashok P, Ganesh Madhan M *Laser Phys. Lett.* **18** 065301 (2021)
12. Pang X et al. *Phys. Status Solidi A* **218** 3 2000407 (2021)
13. Kazarinov R F, Suris R A *Sov. Phys. Semicond.* **5** 707 (1971); *Fiz. Tekh. Poluprovodn.* **5** 797 (1971)
14. Faist J et al. *Science* **264** 553 (1994)
15. Vurgaftman I et al. *J. Phys. D* **48** 123001 (2015)
16. Grillot F et al. *Proc. SPIE* **12430** 1243005 (2023)
17. Meyer J R et al. *Photonics* **7** (3) 75 (2020)
18. Nguyen Van H et al. *Photonics* **6** (1) 31 (2019)
19. Loghmani Z et al. *Appl. Phys. Lett.* **115** 151101 (2019)
20. Loghmani Z et al. *Electron. Lett.* **55** 144 (2019)
21. Wen B, Ban D *Prog. Quantum Electron.* **80** 100363 (2021)
22. Jin Y, Reno J L, Kumar S *Optica* **7** 708 (2020)
23. Kainz M A et al. *Opt. Express* **27** 20688 (2019)
24. Bosco L et al. *Appl. Phys. Lett.* **115** 010601 (2019)
25. Khalatpour A et al. *Nat. Photon.* **15** 16 (2021)
26. Belkin M A et al. *Nat. Photon.* **1** 288 (2007)
27. Lu Q et al. *Nat. Commun.* **10** 2403 (2019)
28. Commin J P et al. *Appl. Phys. Lett.* **97** 3 031108 (2010)
29. Bandyopadhyay N et al. *Appl. Phys. Lett.* **101** 241110 (2012)
30. Bai Y et al. *Appl. Phys. Lett.* **95** 221104 (2009)
31. Heydari D et al. *Appl. Phys. Lett.* **106** 091105 (2015)
32. Slivken S et al. *Appl. Phys. Lett.* **81** 4321 (2002)
33. Bandyopadhyay N et al. *Appl. Phys. Lett.* **105** 071106 (2014)
34. Maulini R et al. *Opt. Express* **19** 17203 (2011)
35. Cherotchenko E et al. *Nanomaterials* **12** 3971 (2022)
36. Xu S et al. *Appl. Phys. Lett.* **121** 171103 (2022)
37. Slivken S et al. *Appl. Phys. Lett.* **80** 4091 (2002)
38. Wang C A et al. *J. Cryst. Growth* **370** 212 (2013)
39. Razeghi M et al. *J. Phys.* **11** 12 125017 (2009)
40. Cristobal E et al. *Appl. Phys. Lett.* **122** 141108 (2023)
41. Wang H et al. *Chinese Phys. B* **30** 124202 (2021)
42. Xie F et al. *IEEE J. Select. Top. Quantum Electron.* **19** 1200407 (2013) <https://doi.org/10.1109/JSTQE.2013.2240658>
43. Huang X, Charles W O, Gmachl C *Opt. Express* **19** 8297 (2011)
44. Fujita K et al. *Appl. Phys. Lett.* **97** 201109 (2010)
45. Szerling A, Slivken S, Razeghi M *Opto-Electron. Rev.* **25** (3) 205 (2017)
46. Babichev A V et al. *Tech. Phys. Lett.* **46** 442 (2020); *Pis'ma Zh. Tekh. Fiz.* **46** (9) 35 (2020)
47. Evans A et al. *Appl. Phys. Lett.* **91** 071101 (2007)
48. Bai Y et al. *Appl. Phys. Lett.* **97** 251104 (2010)
49. Wang F et al. *Opt. Express* **28** 17532 (2020)
50. Babichev A V et al. *Semiconductors* **52** 1082 (2018); *Fiz. Tekh. Poluprovodn.* **52** 954 (2018)
51. Howard S S et al. *IEEE J. Select. Top. Quantum Electron.* **13** 1054 (2007)
52. Babichev A V et al. *Bull. Russ. Acad. Sci. Phys.* **87** 839 (2023); *Izv. Ross. Akad. Nauk. Ser. Fiz.* **87** 855 (2023)
53. Lu Q et al. *Sci. Rep.* **6** 23595 (2016)
54. Dudelev V V et al. *Quantum Electron.* **50** 989 (2020); *Kvantovaya Elektron. Elektron.* **50** 989 (2020)
55. Vruble I I et al. “QCL active region overheat in pulsed mode: effects of non-equilibrium heat dissipation on laser performance,” arXiv:2308.10013
56. Goryunova N A, Kesamanly F P, Nasledov D N *Semicond. Semimet.* **4** 413 (1968)
57. Lee H K et al. *Phys. Status Solidi A* **206** 356 (2009)
58. Gundogdu S et al. *Opt. Express* **2** 6572 (2018)
59. Dudelev V V et al., in *2020 Intern. Conf. Laser Optics, ICLO, 02–06 November 2020, St. Petersburg, Russia*, <https://doi.org/10.1109/ICLO48556.2020.9285842>
60. Dudelev V V et al., in *2019 Conf. on Lasers and Electro-Optics Europe and European Quantum Electronics Conf. CLEO/Europe-EQEC, 23–27 June 2019, Munich, Germany*, <https://doi.org/10.1109/CLEOE-EQEC.2019.8872750>